June 2002

GeV Electrons from Ultraintense Laser Interaction with Highly Charged Ions

S.X. Hu
University of Nebraska - Lincoln

Anthony F. Starace
University of Nebraska-Lincoln, astarace1@unl.edu

GeV Electrons from Ultraintense Laser Interaction with Highly Charged Ions

S. X. Hu and Anthony F. Starace

Department of Physics and Astronomy, The University of Nebraska–Lincoln, Lincoln, Nebraska 68588-0111

(Received 27 September 2001; published 4 June 2002)

Ultraintense laser interactions with highly charged ions are investigated using three-dimensional Monte Carlo simulations. Results show that ultraenergetic GeV electrons may be produced for highly charged ions chosen so that their electrons remain bound during the rise time of the laser pulse, and so that the electrons are ionized when the laser is near its maximum amplitude, which satisfies the best injection condition for subsequent laser acceleration.

DOI: 10.1103/PhysRevLett.88.245003 PACS numbers: 52.38.Kd, 32.80.Fb, 52.65.Pp

Advances in high-power laser technology have resulted in the development of petawatt laser systems [1]. These can deliver superstrong laser pulses, which can be focused to intensities as high as 10^{21} W/cm^2. The physics of the interaction of matter with such strong fields is therefore attracting much attention [2]. Among the key features of this interaction are the production of highly charged ions as well as of fast charged particles, including electrons. For example, intense laser pulses have been found to produce highly charged [3] and energetic [4] ions from clusters. Intense laser interactions with solid targets have been found to produce protons with energies of ≥ 1 MeV [5]. Laser acceleration of electrons in vacuum has been investigated both theoretically [6] and experimentally [7]. It has also been investigated in plasmas [8] owing to possible applications in inertial confinement fusion [9]. Hot electrons with MeV energies have been predicted for atom targets [10], while electrons with energies of a few keV have been observed experimentally for cluster targets [11]. For plasmas, electrons have been observed with energies of a few MeV [12] and theoretical simulations have predicted electron energies of as much as 100 MeV [13]. Recently, Sprangle *et al.* [14] analyzed laser wakefield acceleration of electrons in plasma channels; they predict electron energies of the order of 1 GeV if the laser pulse can propagate a long enough distance in the plasma without disruption. Also, Kimura *et al.* [15] have performed the first experiment on electron accelerators using two intense, coherent lasers acting sequentially on an electron beam.

We analyze here a qualitatively different mechanism for producing high energy electrons in vacuum that involves highly charged ions (HCIs) as targets. On the basis of three-dimensional Monte Carlo simulations, we show that GeV electrons can be generated for particular HCIs and laser parameters. Unlike the relatively weakly bound electrons in neutral atoms, the tightly bound electrons in HCIs may survive the turn-on of an intense laser pulse for a sufficiently strong ionic Coulomb field. When the laser field attains its maximum amplitude, for not too strong an ionic field, an electron may be ionized with sufficient probability. These electrons may then be accelerated by the Lorentz force to relativistic velocities within a small angle about the laser propagation axis. They do this by "riding" on the laser wave, continuing to "see" the maximum field strength of the laser; i.e., they satisfy the phase matching requirements for laser acceleration [15], as shown below.

We consider an ultraintense laser pulse, linearly polarized along the x axis and propagating along the z axis, which is focused to a Gaussian beam having a waist of width w_0. Its electric field is described by

$$\mathbf{E}_L(\rho, z, t) = [E(\rho, z) f(t - z/c) \sin(\omega t - \omega z/c), 0, 0], \tag{1}$$

where the spatial dependence of the field is

$$E(\rho, z) = E_0 \left(\frac{b}{b + 2iz} \right) \exp\left(-\frac{k\rho^2}{b + 2iz} \right). \tag{2}$$

In Eqs. (1) and (2), E_0 is the maximum amplitude of the laser pulse, $k = 2\pi/\lambda$ is the laser wave vector, $b = 2\pi w_0^2/\lambda$ is the confocal parameter, which is related to the beam waist w_0, z is the distance from the focusing center along the laser propagation direction, and ρ is the transverse distance from the z axis. The time envelope $f(t - z/c)$ in Eq. (1) is trapezoidal; it comprises a five-cycle linear turn-on and turn-off, as well as a five-cycle duration at constant amplitude. The laser's magnetic field component, $\mathbf{B}_L(\rho, z, t)$, has a form identical to that of $\mathbf{E}_L(\rho, z, t)$ but along the y axis. For relativistic motion of an electron in both an electromagnetic field and a Coulomb field, the classical dynamics is described by

$$\begin{aligned} d\mathbf{r}/dt &= \mathbf{p}/\gamma, \\ d\mathbf{p}/dt &= -(\mathbf{E}_L + \mathbf{E}_C + \mathbf{p} \times \mathbf{B}_L/\gamma c), \end{aligned} \tag{3}$$

where $\gamma \equiv \sqrt{1 + \mathbf{p}^2/c^2}$ is the relativistic factor in atomic units (used throughout this paper), $c \simeq 137.036$ is the speed of light in vacuum, and $\mathbf{r}$ and $\mathbf{p}$ are the coordinate and the mechanical momentum of the electron, respectively. The Coulomb field is $\mathbf{E}_C = -\nabla V(r)$, where $V(r)$ is the ionic core potential. The Runge-Kutta method with variable step size is used to numerically integrate Eqs. (3). Because these are classical dynamical equations, we are able to trace any particular trajectory that is randomly chosen from a preprepared relativistic microcanonical ensemble for the target ion's ground state. The standard procedure for preparing such an ensemble is as follows [16,17]: (i) In a particular plane, chosen to be

the x-y plane, we solve the relativistic Kepler problem [18] for the ground-state energy and an angular momentum chosen randomly, both of which are conserved quantities of motion; (ii) randomly choosing particular sets of Euler angles (θ, ϕ, η), we then rotate the initial relativistic Kepler orbit into three dimensions. By comparing the radial and momentum distributions of the resulting ensemble of Kepler orbits to the known quantum-mechanical ground-state radial and momentum probability for a hydrogenic ion, we have verified that the microcanonical ensemble truly mimics the quantum-mechanical ground state of interest. This "phase-space-averaging" method [16] has been used extensively to investigate atomic collisions [19], Rydberg atom ionization by microwaves [16], and intense laser-atom processes (see, e.g., Protopapas *et al.* [2], and references therein; also Refs. [10,17]). For the problem considered here, there are two reasons for using the classical Monte Carlo method: (i) A quantum-mechanical calculation is intractable, even in two-dimensions, owing to the large laser-induced excursions made by the ionized electron [20]; (ii) for the highly charged ion and the laser field considered here, tunneling ionization [21] is negligible ($\lesssim 0.1\%$ probability for the pulse turn-on and $\simeq 1\%$ for the entire pulse duration).

In our calculations, the laser wavelength is 1054 nm (as for the hybrid Ti:sapphire-Nd:glass laser system of Ref. [1]), and the laser intensity is 8×10^{21} W/cm^2 when focused to a Gaussian beam with a waist of $w_0 = 10$ μm, as described above. It may seem that, with such an ultraintense laser pulse, the production of ultrahot GeV electrons is not surprising. However, one may show that achieving such energies solely with such an intense laser pulse is not possible: For free electrons at rest as the target, Fig. 1(a) shows that the highest obtainable electron energy as a function of emission angle θ (defined as the angle between the ejected electron and the z axis) is below 200 MeV. In Figure 1(b), we consider a typical trajectory from Fig. 1(a) as a function of time. The solid and dashed lines represent, respectively, the relativistic factor γ for the electron and the laser field strength E_L experienced by the electron, with both plotted as a function of laboratory time along the chosen trajectory. One sees that the electron, initially at rest, is captured and accelerated by the ramping front edge of the laser pulse; then energy is exchanged between the electron and the laser field as the latter oscillates; finally, the electron leaves the laser focusing area before it experiences the peak laser intensity. Because the electron moves relativistically along $\hat{z}$ during its interaction with the laser pulse, the actual interaction time is relativistically modified, and is longer than the pulse duration in the laboratory frame by a factor of $\sim\gamma$. In other words, in the electron frame the laser frequency is significantly redshifted. This is shown in Fig. 1(b) by comparing the oscillation period of γ to the interaction time in the laboratory frame in the region where $\gamma \simeq 380$; they differ by a factor γ.

To keep the electron from being pushed out of the focusing area before "seeing" the peak laser intensity, we

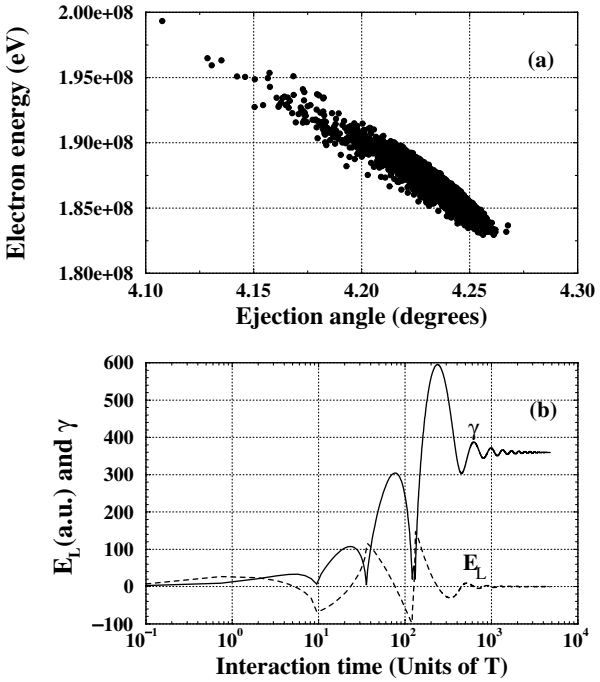

FIG. 1. Three-dimensional Monte Carlo results for the interaction of an ultraintense laser pulse with free electrons initially at rest. The Gaussian laser beam has a wavelength of 1054 nm and a peak intensity of 8×10^{21} W/cm^2. The beam waist is assumed to be 10 μm, and its time envelope comprises a 5-cycle turn-on and turn-off, as well as a 5-cycle flat top with constant amplitude [see Eqs. (1) and (2)]. (a) Electron energy attained as a function of the emission angle θ with respect to the direction of laser propagation. (b) The relativistic factor γ (solid line) for the electron and the laser field strength E_L (dashed line) actually experienced by the electron as a function of the interaction time (in units of $T \equiv 2\pi/\omega$) for a typical electron trajectory.

consider the highly charged hydrogenlike ion V^{22+} as our target. (Nowadays, any charge state of any atom can be produced [22].) Using the three-dimensional Coulomb potential (i.e., $-23/r$ for V^{22+}), the initial relativistic microcanonical ensemble corresponding to the quantum-mechanical ground state (with ionization potential $I_p \simeq 7.2$ keV) was prepared as described above. Some of the 12 000 orbits in our microcanonical ensemble are never ionized, some are ionized "early" during the rise time of the laser pulse, and others are ionized around the peak intensity of the laser pulse (or later). Figure 2 shows the laser field E_L experienced by an electron along both an early and a "peak field" trajectory as a function of time measured in units of the laser period $T \equiv 2\pi/\omega$ in the laboratory frame. One sees that the electron on the early trajectory [Fig. 2(a)] experiences only $\sim$3.75 laser oscillations before being ionized, whereas the one on the peak field trajectory [Fig. 2(b)] experiences $\sim$8.75. The value of E_L experienced by the electron on the early trajectory is significantly lower than that on the peak field trajectory. Nevertheless, both values of E_L are large. What happens following ionization may be summarized succinctly as follows: (i) The electron is accelerated by E_L along the x axis; (ii) the $v_x \times B$ force accelerates the electron

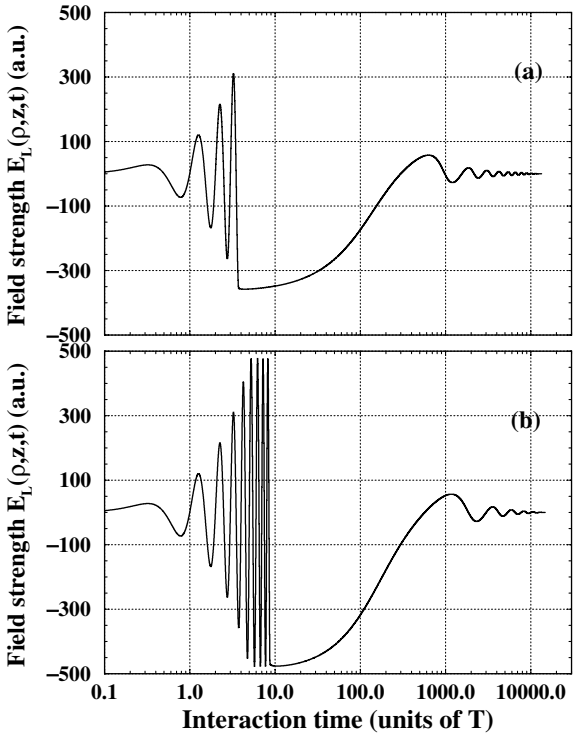

FIG. 2. Instantaneous laser amplitude experienced along a classical relativistic trajectory of an electron initially bound in the highly charged, hydrogenlike ion V^{22+}. (a) Result for one trajectory ionized "early," before the laser pulse maximum. (b) Result for another trajectory ionized at the laser "peak field." The interaction time in the laboratory frame is measured in units of $T \equiv 2\pi/\omega$ on a logarithmic scale.

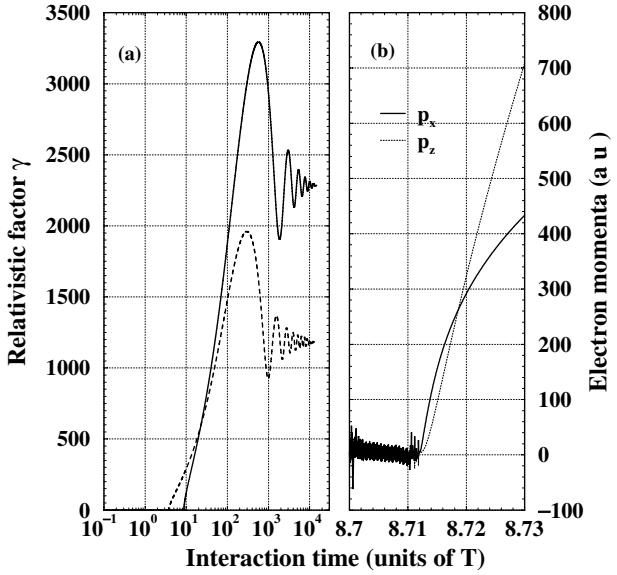

FIG. 3. (a) The relativistic factor γ for the ionized electron plotted vs the interaction time, given in units of T, for the same two classical relativistic electron trajectories shown in Fig. 2, i.e., for "early" ionization (dashed line) and for ionization at the "peak field" (solid line). (b) The evolution of electron momenta just before and after the time of its ionization for the trajectory shown by the solid line in (a).

along the laser propagation direction (z axis); (iii) simultaneously, the $v_z \times B$ component of the Lorentz force acts to reduce the effective acceleration along the x axis. Figure 3(a) shows the relativistic factor γ for each trajectory; Fig. 3(b) shows that for the peak field trajectory the electron momentum component p_z becomes larger than p_x within 0.01 laser period. The entire acceleration occurs effectively within the first quarter of a laser cycle following the electron's ionization; i.e., in its rest frame, the electron "rides" on the peak laser field with only a small phase slippage (because $v_z \lesssim c$). Note also that, by reducing the effective field along the x axis, the $\mathbf{v} \times \mathbf{B}$ force efficiently confines the transverse motion of the electron so that it remains inside the focusing area. The net result is that the greater the $\mathbf{v} \times \mathbf{B}$ force, the larger the electron's momentum p_z relative to p_x and, hence, the smaller the electron's angle of ejection relative to the z axis. That the acceleration of the electron on either trajectory occurs in the quarter of a laser period (in the electron rest frame) following the electron's becoming free of the Coulomb potential of the ion can be seen in Fig. 3(a). The electron accumulates energy from the laser pulse during the quarter of a laser period in which the relativistic electron continues to "see" the laser field amplitude with the same sign (i.e., from $\simeq 4T$ to $\simeq 298T$ on the early trajectory and from $\simeq 9T$ to $\simeq 570T$ on the peak field trajectory). When the field changes its sign (due to phase slippage), the electron is decelerated, resulting in a loss of electron energy. However, since the electron is simultaneously being pushed out of the focusing area, the laser field turns out to be much weaker then. Thus, the energy loss by the electron is slight, and does not offset the prior energy gain. After several such oscillations, the electron completely escapes from the focusing area with a constant energy of $\simeq 1.2$ GeV ($\simeq 600$ MeV) for the peak field (early) trajectory.

Results for final electron energies obtained from three-dimensional Monte Carlo simulations for a V^{22+} ion at $\rho = 0$ are shown in Fig. 4. Figure 4(a) gives the distribution of attained electron energy as a function of ejection angle for each of the 4000 ionizing trajectories (a total of $\sim$12 000 trajectories are considered; $\simeq 33\%$ of them result in ionization). The closer to the laser propagation axis the electron is ejected, the more energetic it is, since a smaller ejection angle implies a longer path within the focusing area. The energy distribution of the ejected electrons is shown in Fig. 4(b), in which the histogram having the largest number of trajectories (located at about 1.01 GeV) is normalized to unity. Nearly 60% of the ionized electrons have an energy $\gtrsim$1.0 GeV. The maximum electron energy for the case of V^{22+} is about 1.8 GeV. Spatial averaging over the central focal region ($0 \leq \rho \leq 2$ μm) results in $\gtrsim$30% ionization with $\gtrsim$30% of the ionized electrons exceeding 1 GeV.

There are many parameters which may be varied, some of whose effects we have examined. Similar calculations for a Gaussian laser temporal pulse shape give similar

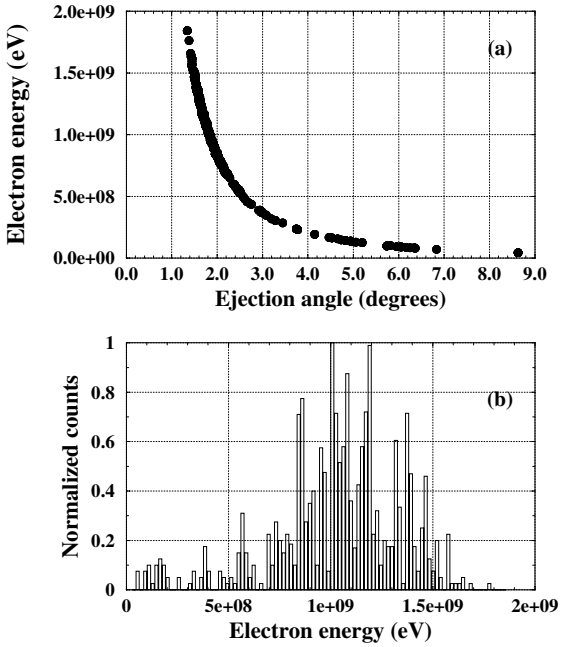

FIG. 4. Three-dimensional Monte Carlo simulation results for V^{22+} located at the center of the laser pulse described in the text. (a) Electron energies attained vs the ejection angles with respect to the z axis. (b) Electron energy distribution normalized to the peak of the distribution.

results. Increasing the pulse duration by a factor of 5 for V^{22+} at $\rho = 0$ results in nearly 100% ionization (but only about 5% by tunneling) with nearly half the electrons achieving energies ≥ 1 GeV. For Cr^{23+} ($I_p = 7.836$ keV), about 10% of the electron trajectories are ionized for the same short laser pulse as for V^{22+}. We note that neonlike xenon (Xe^{44+}) has an ionization energy of 7.664 keV [23], which lies between those for V^{22+} and Cr^{23+}. However, many-electron effects may be important for Xe^{44+}.

In summary, appropriately selected HCIs may be an efficient source of electrons for subsequent ultraintense laser acceleration. For any laser field under consideration, the binding energy of the active electron in the HCI should be sufficiently high that ionization by tunneling during the rise time of the laser pulse is negligible, but not so high that the classical ionization probability at the peak laser intensity is small. Generally, there is a range of HCIs that will satisfy these requirements. For the HCI meeting these criteria, electrons that are ionized may be sufficiently relativistic to satisfy the optimum injection conditions for subsequent laser acceleration. Namely, these relativistic free electrons can ride on the propagating laser wave and see the laser's maximum field strength while being accelerated so that energies of the order of 1 GeV can be achieved, as we have demonstrated for the particular example of V^{22+} and a short pulse with an intensity of 8×10^{21} W/cm^2. Experimentally, highly charged ions may be produced either by employing a laser prepulse [3] or by various electronic, atomic, or ionic collision processes [22]. A double-pulse scheme may also be feasible by splitting a laser pulse into two subpulses, one of which is used to ionize clusters or solids, and the other of which is delayed so that it interacts directly with these HCIs.

Note added: After submission of this Letter, we became aware of schemes to produce GeV electrons by injecting fast electrons into a laser focus [24].

We thank N. L. Manakov for helpful discussions. This work was supported in part by DOE Office of Science, Division of Chemical Sciences, Grant No. DE-FG03-96ER14646.

[1] M. D. Perry *et al.,* Opt. Lett. **24**, 160 (1999).
[2] G. A. Mourou *et al.,* Phys. Today **51**, No. 1, 22 (1998); M. Protopapas *et al.,* Rep. Prog. Phys. **60**, 389 (1997); P. Salières *et al.,* Adv. At. Mol. Opt. Phys. **41**, 83 (1999); T. Brabec and F. Krausz, Rev. Mod. Phys. **72**, 545 (2000).
[3] T. Ditmire *et al.,* Phys. Rev. Lett. **75**, 3122 (1995); E. M. Snyder *et al.,* Phys. Rev. Lett. **77**, 3347 (1996).
[4] T. Ditmire *et al.,* Nature (London) **386**, 54 (1997); Phys. Rev. A **57**, 369 (1998).
[5] E. L. Clark *et al.,* Phys. Rev. Lett. **84**, 670 (2000); A. Maksimchuk *et al., ibid.* **84**, 4108 (2000).
[6] F. V. Hartemann *et al.,* Phys. Rev. E **51**, 4833 (1995); B. Quesnel and P. Mora, Phys. Rev. E **58**, 3719 (1998); J. X. Wang *et al.,* Phys. Rev. E **60**, 7473 (1999); Y. I. Salamin and F. H. M. Faisal, Phys. Rev. A **61**, 043801 (2000); Y. I. Salamin, F. H. M. Faisal, and C. H. Keitel, Phys. Rev. A **62**, 053809 (2000).
[7] G. Malka *et al.,* Phys. Rev. Lett. **78**, 3314 (1997).
[8] P. Sprangle *et al.,* Appl. Phys. Lett. **53**, 2146 (1988); A. Ting *et al.,* in *Advanced Accelerator Concepts,* edited by Chan Joshi, AIP Conf. Proc. No. 193 (AIP, New York, 1989), p. 398; K. Nakajima *et al.,* Phys. Rev. Lett. **74**, 4428 (1995); E. Esarey *et al.,* IEEE Trans. Plasma Sci. **24**, 252 (1996); F. Amiranoff *et al.,* Phys. Rev. Lett. **74**, 5220 (1995); F. Dorchies *et al.,* Phys. Plasmas **6**, 2903 (1999).
[9] M. Tabak *et al.,* Phys. Plasmas **1**, 1626 (1994).
[10] C. H. Keitel, J. Phys. B **29**, L873 (1996).
[11] Y. L. Shao *et al.,* Phys. Rev. Lett. **77**, 3343 (1996).
[12] X. Wang *et al.,* Phys. Rev. Lett. **84**, 5324 (2000).
[13] W. Yu *et al.,* Phys. Rev. Lett. **85**, 570 (2000).
[14] P. Sprangle *et al.,* Phys. Rev. Lett. **85**, 5110 (2000).
[15] W. D. Kimura *et al.,* Phys. Rev. Lett. **86**, 4041 (2001).
[16] J. G. Leopold and I. C. Percival, Phys. Rev. Lett. **41**, 944 (1978); J. Phys. B **12**, 709 (1979).
[17] H. Schmitz *et al.,* Phys. Rev. A **57**, 467 (1998).
[18] R. D. Sard, *Relativistic Mechanics* (Benjamin, New York, 1970).
[19] R. Abrines and I. C. Percival, Proc. Phys. Soc. London **88**, 861 (1966); **88**, 873 (1966); R. E. Olson and A. Salop, Phys. Rev. A **16**, 531 (1977); J. S. Cohen, *ibid.* **26**, 3008 (1982).
[20] S. X. Hu and C. H. Keitel, Phys. Rev. A **63**, 053402 (2001).
[21] A. M. Perelomov *et al.,* Sov. Phys. JETP **23**, 924 (1966); M. V. Ammosov *et al.,* Sov. Phys. JETP **64**, 1191 (1986).
[22] J. D. Gillaspy, J. Phys. B **34**, R93 (2001).
[23] Kh. U. Zibert *et al.,* Opt. Spectrosc. (USSR) **42**, 584 (1977).
[24] See Y. I. Salamin and C. H. Keitel, Phys. Rev. Lett. **88**, 095005 (2002), and references therein.